(1)

OFFICE OF NAVAL RESEARCH
GRANT N00014-94-I-0331

R & T Code 4133044
Robert Nowak

Technical Report No. 67

Angle Resolved Auger Electron Spectroscopy: An Alternate Tool For Identifying Electronic Excitation Processes In Solids

by

D.E. Ramaker, R.A. Fry, and Y.U. Idzerda

Prepared for Publication

in the

Journal Electron Spectroscopy and Related Phenomena

George Washington University
Department of Chemistry
Washington, D.C.

September 1994

REPORT DOCUMENTATION PAGE

Form Approved
OMB No. 0704-0188

1. AGENCY USE ONLY (Leave blank)	2. REPORT DATE	3. REPORT TYPE AND DATES COVERED
	September 1994	Technical Sept'93-Oct'94

4. TITLE AND SUBTITLE
Angle Resolved Auger Electron Spectroscopy: An Alternate Tool for Identifying Electronic Excitation Processes in Solids

5. FUNDING NUMBERS
Grant #:
N00014-94-I-0331
Robert Nowak, Prog Off
R & T: 4133044

6. AUTHOR(S)
D.E. Ramaker, R.A. Fry, and Y.U. Idzerda

7. PERFORMING ORGANIZATION NAME(S) AND ADDRESS(ES)
Chemistry Department
George Washington University
Washington, D.C. 20052

8. PERFORMING ORGANIZATION REPORT NUMBER
Technical Report
#67

9. SPONSORING/MONITORING AGENCY NAME(S) AND ADDRESS(ES)
Office of Naval Research
800 N. Quincy Street
Arlington, VA 22217-5000

10. SPONSORING/MONITORING AGENCY REPORT NUMBER

11. SUPPLEMENTARY NOTES

12a. DISTRIBUTION/AVAILABILITY STATEMENT
Approved for public release; distribution is unlimited.

12b. DISTRIBUTION CODE
Approved for public release and sale; distribution is unlimited

13. ABSTRACT *(Maximum 200 words)*

Angle resolved Auger electron spectroscopy (ARAES) is shown to be a useful tool for obtaining unique electronic structure information and identifying "satellite" excitation processes in solids. Although relatively unexplored, ARAES is an attractive tool which may complement the more conventional energy resolved AES. The ARAES method is successful because the diffraction patterns exhibited in ARAES at fixed energy are strongly dependent on the ℓ-wave of the emitted electron and its magnetic alignment, and each Auger process is generally dominated by a different single ℓ-wave. Potential applications for elucidating satellite excitation processes (resonant excitation, shakeup/shakeoff, and backscattering), one- and two-center decay processes, and electronic structure (directional valence bonds and orbital magnetic moments) at surfaces are discussed.

14. SUBJECT TERMS
Auger Spectroscopy, ARAES, Transition Metals, Diffraction

15. NUMBER OF PAGES

16. PRICE CODE

17. SECURITY CLASSIFICATION OF REPORT	18. SECURITY CLASSIFICATION OF THIS PAGE	19. SECURITY CLASSIFICATION OF ABSTRACT	20. LIMITATION OF ABSTRACT
Unclassified	Unclassified	Unclassified	Unlimited

Angle resolved Auger electron spectroscopy: an alternate tool for identifying electronic excitation processes in solids *

D.E. Ramaker[abc], R.A. Fry[a], and Y.U. Idzerda[c]

[a]Materials Science Institute and
[b]Chemistry Department, George Washington University, Washington, DC 20052
[c]Naval Research Laboratory, Washington, DC 20375

Angle resolved Auger electron spectroscopy (ARAES) is shown to be a useful tool for obtaining unique electronic structure information and identifying "satellite" excitation processes in solids. Although relatively unexplored, ARAES is an attractive tool which may complement the more conventional energy resolved AES. The ARAES method is successful because the diffraction patterns exhibited in ARAES at fixed energy are strongly dependent on the ℓ-wave of the emitted electron and its magnetic alignment, and each Auger process is generally dominated by a different single ℓ-wave. Potential applications for elucidating satellite excitation processes (resonant excitation, shakeup/shakeoff, and backscattering), one- and two-center decay processes, and electronic structure (directional valence bonds and orbital magnetic moments) at surfaces are discussed.

1.INTRODUCTION

Considerable success has been achieved utilizing X-ray photoelectron diffraction and Auger electron diffraction (XPD and XED) to characterize ultra-thin films and overlayers in determining the structure [1,2,3], the film growth mode [4,5], and to resolve surface reconstructions [6]. The applicability of these techniques has expanded rapidly, to include even more complex systems such as surface melting, ion-induced amorphization, surface segregation etc. [7]. The number of recent reviews indicates the work level in this area [1-3,7,8].

In spite of this activity, quantitative understanding of the intensity patterns is still often lacking; even after utilization of the quantum mechanical scattering codes. Most often the discrepancy between the theoretical scattering results and experiment has been attributed to a non-spherical Auger source, or in other words to a non-uniform population of the magnetic quantum states, m_ℓ, of an individual ℓ wave characterizing the emitted electron [9,10,11,12,13]. The populations of ℓ and m_ℓ constitute what is called the "basic structure" of the emitter [14] or what we shall call the "emitter structure". It can be relatively simply determined from the experimental ARAES data, since at lower kinetic energies, the scattering depends strongly on ℓ [4,15,16], and m_ℓ is directly revealed in the asymmetry of the ARAES patterns.

What has not been generally realized is that the emitter structure is a window on the surface electronic structure and electronic excitation processes in solids. The alignment of the emitter structure can provide information on directed valence bonds or orbital magnetic moments at the surface. The "satellite" excitation processes (such as resonant excitation, shakeoff, backscatter excitation, and other excitation processes) can often be distinguished from the

*Support from the Office of Naval Research is gratefully acknowledged.

"principal" Auger decay process in solids, because each Auger decay process is generally dominated by a different single ℓ-wave [15,17]. Thus different excitation processes, which may not be resolved in energy resolved AES (ERAES), can at times be differentiated in angle-resolved AES (ARAES).

We shall refer to an examination of the emitter structure as ARAES, as opposed to AED, when the determination of the atomic structure is the priority. After a brief introduction on the experimental procedures utilized and on the theory, we shall consider the following potential ARAES applications:

1) determine backscattering factors
2) isolate resonant satellites
3) resolve multiplet structure
4) uncover many-body satellites
5) probe directional valence bonds.
6) detect two-center Auger processes
7) estimate orbital magnetic moments.

2.EXPERIMENTAL

All of the experimental data utilized in this work have been previously reported in the literature over the last 15 years [9-13,18,19]. In all cases the incident energy, E_i, and angle, θ_i, are held constant. This is in contrast to other recent work where the incident beam direction is varied, sometimes referred to as directed AES (DAES) [20] or primary beam AES (PBAES) [7], where the incident beam exhibits its own diffraction effects incoherently from the Auger electron beam. E_i and θ_i are reported in the figures below because they determine the relative magnitude of the secondary electron contribution, which is important in the backscattering effect. We assume here that the signals reported indeed come only from the Auger electrons. One geometrical factor arising from the experimental setup is the Lambert factor $\cos(\theta-\theta_0)$ [13c], which arises because the acceptance area by the analyzer at polar angles larger than θ_0 is larger than the excitation beam cross-sectional area. We have multiplied the theoretical polar scans by $\cos\theta$ since we have no knowledge of θ_0.

3.THEORY

3.1.Electron diffraction

In this work, we utilize Fadley's curved wave-single scattering cluster (CW-SSC) code to perform the diffraction calculations [2,21]. Fadley's SSC code is based on the Rehr-Albers formalism which calculates the differential electron yield

$$d\sigma/d\Omega \quad \propto \quad \Sigma[\ell] \quad |M_\ell(k)|^2, \qquad (1)$$

(for clarity here we ignore Debye-Waller and inelastic loss factors, and broadening effects) where $d\sigma/d\Omega$ corresponds to the total electron yield in direction k. The notation $\Sigma[\ell]$ indicates sum over ℓ, and in general, only one term in this sum is large. $|M_\ell(k)|^2$ can be expressed as [21]

$$|M_\ell(k)|^2 \quad \propto \quad \Sigma[m_\ell,m_\ell'] B_\ell(m_\ell,m_\ell') \times [Y_\ell(m_\ell,k) + \Sigma[j] \quad \phi_j(\ell,m_\ell)]^* \times [Y_\ell(m_\ell',k) + \Sigma[j] \quad \phi_j(\ell,m_\ell')], \qquad (2)$$

where $Y_\ell(m_\ell,k)$ is the spherical harmonic, which describes the angular behavior of the electron as it leaves the emitter, and $\Sigma[j]$ $\phi_j(\ell,m_\ell)$ is the net result of scattering from n scatterers at sites r_j (j=1 to n) in the cluster. Here $B_\ell(m_\ell,m_\ell')$ is the photoelectron or Auger amplitude which determines the relative magnitude of each m_ℓ and m_ℓ'. In this work we consider only ARAES when $B_\ell(m_\ell,m_\ell')$ is the emitter structure.

The effects of multiple-scattering (MS) on the diffraction patterns have been examined extensively for the metals considered here, namely Ni, Cu, Al, and Fe. Generally, the effects of MS are to decrease the extent of forward scattering, because of the defocussing effect. It has been found that the SSC code can mimic the defocussing effect by decreasing the inelastic mean free path, λ, by about a factor of two [21b]. In this work, the Auger energies are below 300 eV, so we utilize a λ of 3 Å for all calculations reported here, except where noted.

3.2. Determination of $B_\ell(m_\ell,m_\ell')$

To characterize $B_\ell(m_\ell,m_\ell')$, one can expand the angular momentum distribution into multipole moments [22]

$$B_\ell(m_\ell,m_\ell') = \Sigma[kq]\ \langle J^k_q\rangle\ (-1)^{**}(\ell-m_\ell)\ x \begin{bmatrix} \ell & k & \ell \\ m_\ell & q & m_\ell' \end{bmatrix}, \qquad (3)$$

where the [ ] indicates the 3j symbols, and $k < 2\ell$ and $-k < q < k$. All odd multipoles (k odd; dipole, octupole, etc.) describe the orientation of ℓ, i.e. which way ℓ points regarded as a single-headed arrow, and all even multipoles (quadrupole, etc.) describe the alignment of ℓ as a double-headed arrow. If all multipoles except the monopole are zero, the distribution is isotropic, and all the m_ℓ are equally populated. Orientation corresponds to a preferential population of some m_ℓ versus $-m_\ell$. Alignment corresponds to a preferential population of $\pm m_\ell$ compared with $\pm m_\ell'$ [22]. We will refer to $\langle j^1_0\rangle/\langle j^0_0\rangle$ and $\langle j^2_0\rangle/\langle j^0_0\rangle$ as the orientation, $O(\ell)$, and alignment, $A(\ell)$, respectively. In summary, if the $2\ell+1$ m_ℓ populations are listed in order from $-\ell$ to $+\ell$, $O(\ell) > 0$ ($O(\ell) < 0$) corresponds to increasing (decreasing) m_ℓ populations, $A(\ell) < 0$ ($A(\ell) > 0$) to a "valley" ("peak") distribution where m_0 is the minimum (maximum).

Extensive work has been done to determine $B_\ell(m_\ell,m_\ell')$ for Auger emission in free atoms excited by electrons [23,24,25,26], protons [27], or photons (plane and circularly polarized) [28,29]. For an unpolarized target and unpolarized incoming beam, and assuming the quantization axis (the z-axis) is along the beam direction, $\langle J^k_q\rangle = \langle J^k_q\rangle \sigma_{q0}\sigma_{k,odd}$, i.e. $B_\ell(m_\ell,m_\ell')$ is diagonal, and we have only an alignment of the magnetic levels. Furthermore, $\langle J^k_q\rangle$ for $k > 2$ is very small, so that $A(\ell)$ can be factored into the alignment of the core level, A(L), times the Auger effect, $A(\ell) = \alpha_2 A(L)$ [30].

Several experimental and theoretical studies on the variation of the core ion alignment, A(L), with electron excitation have appeared in the literature [23-26,30]. In general, at high impact energy (10-50 times the threshold energy), the dipole selection rule ($\Delta\ell = \pm1$ and $\Delta m_\ell = \pm1$) holds. Since $I_{\ell+1}$ usually dominates at high energies, A(L) decreases to zero. At threshold energies, the lower ℓ values dominate and the rule $\Delta m_\ell = 0$ takes over. In this case A can be large. Thus experiment and theory indicate a large A(L) at threshold which generally decreases with beam energy.

Expressions of the form

$$\alpha_2 = \Sigma[i]\{a_i M^2_{Lf+i} + a_{-i} M^2_{Lf-i} + a_{i,-i} M_{Lf+i} M_{Lf-i} \cos\Delta_{i,-i}\} / \Sigma[i]\{b_i M^2_{Lf+i} + b_{-i} M^2_{Lf-i}\} \qquad (4)$$

have been derived by Kabachnik and Sazhina [30]. They have tabulated the a and b coefficients for the $p_{3/2}$ ($A = 0$ for the $p_{1/2}$ case), $d_{5/2}$ and $d_{7/2}$ initial core and $^{2S+1}\{Lf\}_J$ Auger final states assuming the usual mixed coupling scheme (jj initial and LS final). Here the M_{Lf} are the Auger decay amplitudes when represented in the form $M_{Lf}\exp(i\sigma_{Lf})$ for $Lf + \ell = L$, $\Delta_{i,-i}$ is the phase shift difference $\sigma_{Lf-i} - \sigma_{Lf+i}$, and L and Lf are the total orbital angular momentum of the initial core ion and the Auger final state, respectively. When a single channel dominates (which is most often the case here), α_2 is independent of the M values and it can be obtained directly from the a's and b's tabulated [30]. We will utilize these in our analyses below.

The situation for ARAES from a solid is now best summarized by Fig. 1. The electron beam generally comes in at an oblique angle with beam energy typically from 1-2 keV. The very low binding energy of the M_{23} core levels (typically 55 to 65 eV for Cu, Ni, and Fe studied here), allows these levels to be excited by the large number of low energy secondary electrons resulting from the cascade and energy loss process. The

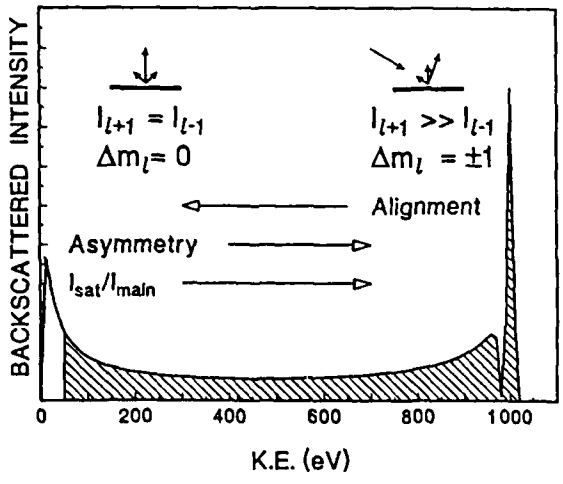

Figure 1. Illustration of the backscattered electron intensity as a result of a 1000 eV electron beam. The shaded area indicates flux of electrons which can excite a core level with a binding energy of 50 eV. Arrows indicate that the alignment of the core level increases and the asymmetry decreases with electron excitation energy as a result of the selection rules for electron ionization as indicated. The relative satellite intensity increases with excitation energy consistent with the "sudden" approximation.

redistributed electrons at higher energy have some memory of the beam angle. However, the true secondary electrons "forget" the direction of the initial electron or photon beam. Their distribution is determined primarily by the preferred transmission direction in the solid, and is assumed to be axially symmetric about the surface normal, which we now make the quantization axis. Since the $<J^k_q>$ are spherical tensors, we can rotate the z-axis from the beam direction to the surface normal utilizing the well-known rotation matrices, $D^2_{qq'}$ [21], giving $<J^k_q>^s = D^2_{q0}\, A^b(L)$, where we have noted the multipoles relative to the surface normal by superscript "s" and to the beam direction now by "b". Note that $<J^k_q>^s$ for $q \neq 0$ are now finite, so that the B matrix is now not diagonal and an anisotropy exists. We conclude that excitation by the primary or redistributed primaries can introduce an anisotropy in B (i.e. $p_1 \neq p_{-1}$), while the lower energy true secondaries introduce an alignment (i.e. $p_0/p_{\pm 1} >> 1$) in B as summarized in Fig. 1.

4.POTENTIAL APPLICATIONS

4.1.Determine backscattering factors

Figure 2 shows experimental $M_{23}VV$ ARAES data for Cu from various surfaces [11,13,31,32], where the reduced intensity in the forward directions at these low energies is clearly evident from the minima at 0^o (100), 19.5^o (302) and 45^o (101) in the <100> azimuth, and at 35^o (211) in the <011> azimuth. We have shown similar data for Ni previously [17]. Figure 2 also shows a significant dependency on energy and incidence of the excitation beam; indeed with increasing beam energy and closer to normal incidence (the latter apparently more important), the more depressed the Auger signal is in the normal direction compared with the theory. We attribute this to the increasing magnitude of low energy secondary electrons with beam energy and normal incidence. For the $\ell = 3$ Auger wave, which dominates for the Ni and Cu $M_{23}VV$ transition, $A(\epsilon f)/A(3p)$ is large and negative. Since the secondary electron excitation process preferentially populates the p_0 level (negative A(3p)), this means the Auger process preferentially populates the $f_{\pm 3}$ (i.e. positive A in the f levels). This introduces a strong reduction in the normal direction, the direction the f_0 electrons would predominantly escape; indeed f_0 is the only wave with any intensity along the z-axis. This suggests the real possibility of determining the backscattering contribution from the extent of alignment seen in the ARAES. Knowledge of these backscattering factors is essential in quantitative Auger applications.

4.2.Isolate resonant satellites

Fig. 2 also shows the M_1VV ARAES yield from Cu(100) and comparison with the yield

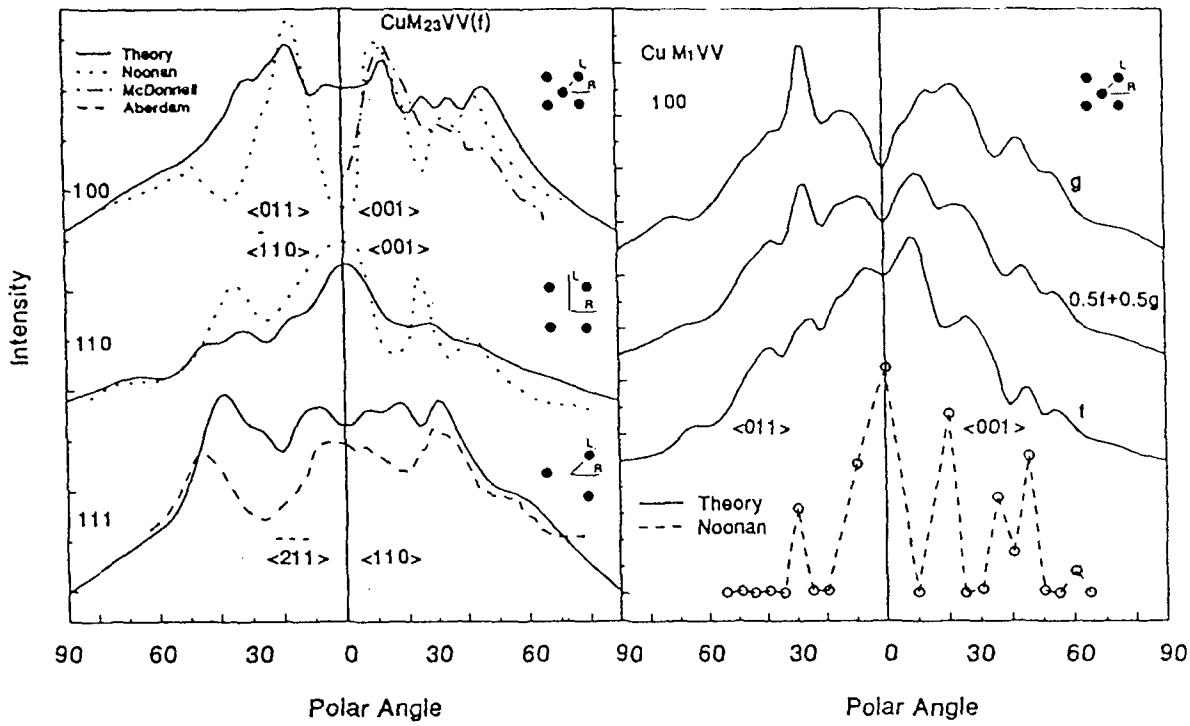

Figure 2. Comparison of theoretical and experimental polar scans for Cu $M_{23}VV$ and M_1VV from various surfaces. The theoretical scans are obtained from the CW-SSC code utilizing $\ell = 3$ for the $M_{23}VV$ and $\ell = 4$ (equal m_ℓ) and 3 (relative populations = 1, 4.1, 6.0, 6.6 for $m_\ell = \pm 3$, ± 2, ± 1, and 0, respectively [17]) for M_1VV. Experimental data from Noonan et al. (E_i = 350 eV, $\theta_i = 0^o$) [12c] and McDonnell et al. (E_i = 1500 eV, θ_i = ?) [9a] for Cu (100), Zehner et al. (E_i = 350 eV, θ_i = 0-30^o) [12a] for Cu(110), and McDonnell et al. (E_i = 1500 eV, θ_i = ?) [9a] for Cu(111). The M_1VV experimental data are obtained from Noonan et al. [12c] who, because of the very weak signal involved, reported a small number of experimental points.

calculated for $\ell = 4$, the expected dominant ℓ wave in this instance [33]. Note that a strong enhancement is now evident in the normal direction, in contrast to that found for the calculated g wave and in contrast to that for the $M_{23}VV$ yield from the (100) surface. Obviously, this cannot arise from an alignment in the M_1 (3s) core level ($m_\ell = 0$ only); but excitation of the 3s level in Ni or Cu is known to exhibit significant many-body effects (i.e. shakeup or shakeoff satellites in the XPS spectra) [34], and also to exhibit a resonant 3s → 4p photoemission process at threshold in Ni [35]. The 3s → 4p transition at threshold decays via the direct recombination and Auger processes,

$$3s^2 3p^6 3d^9 4s^1 \rightarrow 3s 3p^6 3d^9 4s^1 4p^1$$

$$\rightarrow 3s^2 3p^6 3d^8 4s^1 + \epsilon f$$

$$\rightarrow 3s^2 3p^6 3d^7 4s^1 4p^1 + \epsilon g,$$

where the former resonates with the direct 3d emission

$$3s^2 3p^6 3d^9 4s \rightarrow 3s^2 3p^6 3d^8 4s + \epsilon f.$$

We believe the threshold secondary electrons are resonantly exciting into the 3s → $4p_0$ state

(i.e. $m_\ell = 0$ since $\Delta m_\ell = 0$ at low energy), and the direct recombination results in $\ell = 3$, but very strongly aligned (negatively). The aligned f wave (with m_ℓ populations strongly peaked toward f_0 as indicated in Fig. 2) is strongly peaked in the normal direction. The resonant Auger decay (i.e. $4p_0$ as spectator) is indistinguishable from the normal Auger decay since both give a non-aligned g wave. Although the direct recombination contribution is expected to be shifted by ≈4 eV from the Auger signal, the 10 V_{ptp} modulation used to collect the extremely weak signal, indicates that the Auger, resonant Auger, and direct contributions are not energetically resolved here. Fig. 1 reveals that a combination of the aligned f and non-aligned g waves give satisfactory agreement with experiment and again shows the dominant excitation by low energy secondary electrons, and the clear presence of a resonant contribution, which was not evident in the ERAES.

One might ask why a similar process does not occur in the $M_{23}VV$ case for Cu. In this case the resonant process would be $3p_0 \rightarrow 4s$, followed by 2p3d4s decay which gives a dominant p wave with in fact a small positive alignment (i.e. $p_0 \approx p_{\pm 1}$).

4.3.Resolve multiplet structure

Calculations show that the different $^{2S+1}\{Lf\}_J$ final state multiplets have widely different α_2 factors, so that the same ℓ-wave from different multiplets should exhibit different alignments [30]. If these multiplets are energetically separated (although not necessarily resolved), such as in Cu, different ARAES patterns should be obtained for each multiplet (i.e. the "basic structure" should change with energy.)

Recently, Mroz and Stachnik have shown for Cu and Ni that various ARAES polar scans do indeed change with electron kinetic energy across the Auger energy spectrum [36]. Fig. 3 summarizes this data for different surfaces, by taking the ratio of the intensity at different polar angles, I_o/I_x, where I_o signifies the intensity in the normal direction, and I_x is generally a nearby intensity peak at x degrees from the normal. In the case of Cu(110), an asymmetry in the data around 11^o on either side of the normal (I_{11}/I_{-11}) was found to change with energy.

These changes can arise from two different sources. The most obvious of these is from changes in the wavevector k with kinetic energy, but such changes are expected to be small since k is changing by less than 10% in this energy range (53-64 eV). Furthermore, the changes are seen mostly near the normal, where the effects of the alignment of the ℓ-wave are most pronounced. The change in I_{11}/I_{-11} cannot arise from changes in k, since pure scattering effects would require this ratio to be unity, and the 110 face is symmetric about this azimuth. The changes seen are believed to reflect changes in the "basic structure" of the Auger wave.

In Fig. 3, we show the Auger spectral lineshape Mroz and Stachnik obtained by simply removing an approximate extrapolated background [36]. We compare this lineshape with that obtained by Sickafus and Kukla [37] which has all inelastic losses removed by deconvolution from the lineshape. We also show vertical lines obtained from Roberts et al. [38], which reflect individual multiplets resolved in a high resolution spectrum for the Cu L_3VV lineshape. Since the L_3VV and M_3VV lineshape must exhibit the same final states, we can use these lines to predict the $M_{23}VV$ lineshape. The ^1G and ^3F multiplets dominate the spectrum along with multiplets at lower energy due to a L_3V-VVV satellite arising from the Coster-Kronig and shakeoff processes. This comparison allows us to determine that electrons below 60 eV reflect satellite and inelastically scattered Auger electrons, those at 61.5 eV mainly ^1G, and those around 64 eV, ^1G plus ^3F final states. Data for the Ni lineshape are similar [39].

Except for the I_{11}/I_{-11} curve for Cu(110), the intensity ratios are relatively flat across the loss and satellite region, as expected. These ratios are widely different for the ^1D and ^3F electrons, but surprisingly in opposite directions for the Ni(111) vs. the other surfaces. Calculations indicate that f_0/f_i should be less than unity for the ^1G and

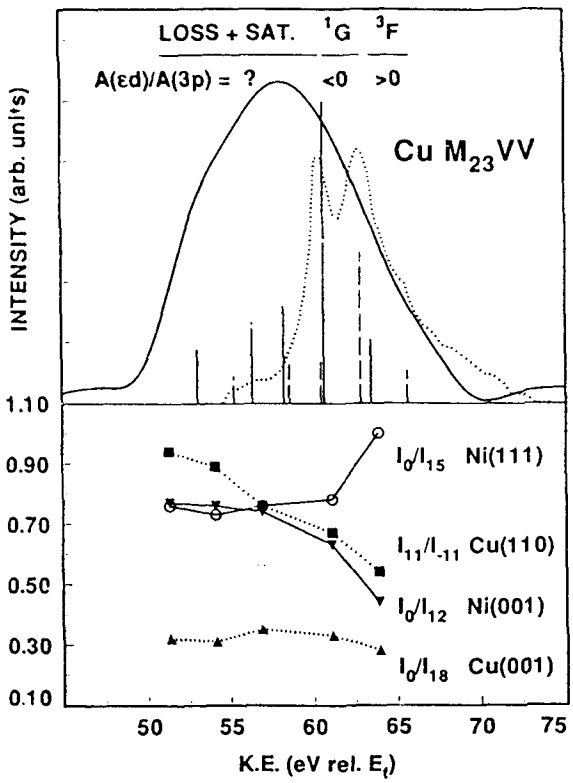

Fig. 3. Top: The background subtracted spectrum of Mroz and Stachnik [36] (solid) is compared with the background subtracted and loss deconvoluted spectrum of Sickafus and Kukla [37] (dotted). Vertical lines indicate the position and relative intensity of ^1G and ^3F multiplet peaks plus several "loss + sat" peaks as found by Roberts et al [38] in a high resolution Cu $L_{23}VV$ lineshape. The solid (dotted) vertical lines indicate the M_3 (M_2) contributions assuming an energy separation of 2.7 eV and relative intensity of 2/1. The sign of the alignment ratio $A(\epsilon d)/A(3p)$ is indicated. Bottom: A plot of I_x/I_y as defined in the text vs. Auger kinetic energy across the Cu $M_{23}VV$ lineshape.

greater than unity for the ^3F final states [30], consistent with the data for Ni(111), but not for Cu(110) and Ni(001). Obviously more careful data needs to be taken to settle these issues, but the data do suggest that such studies can be done to "resolve" multiplet structure.

4.4.Uncover many-body satellites

4.4.1.Valence level shakeoff in Al

It is known from energy resolved Auger studies, that a large probability exist for shakeoff from the Al 3s shell [40] upon sudden creation of a core hole. Since the $M_{23}3s3p$ decay results in a dominant s Auger wave, we expect increased s wave character with decreased shakeoff; i.e. increased s wave character arises with increased low energy excitation resulting from the threshold secondary electrons. We have shown previously that this shakeoff is more evident in the Al ARAES data than in the energy resolved Auger data. ARAES data confirms the large 3s shakeoff which occurs upon sudden creation or filling of the core hole. This phenomenon has been discussed often in the literature for Mg, Al, and Si; these three solids show the reduced ss and sp valence band hole contributions in the ERAES. ARAES can help to uncover these satellites here and perhaps in other cases.

4.4.2.Core-level shakeoff in Al

Recently Greber et al. [4c] reported experimental full 2π 1s photoelectron and Al $L_{23}VV$ normal and L_{23}^2-$L_{23}VV$ satellite Auger electron distributions for Al(001). Because Greber et al excited the Auger spectra utilizing an experimental setup which had the incoming photons coming at an oblique angle with respect to the plane defined by the surface normal and the detector, they observed a mirror-symmetry breaking in the angular distribution of the 1s XPS. A significant asymmetry was still present in the L_{23}^2-$L_{23}VV$ case, but nearly negligible in the $L_{23}VV$ case. They [4c] obtained reasonable agreement with experiment and a least squares fit of SSC code results for individual ℓ contributions including ℓ = s, p, and d. For the $L_{23}VV$ Auger emission at 70 eV, they found the s:p:d ratio to be 0.24:0.26:0.50 and for the L_{23}^2-$L_{23}VV$ satellite emission at 85 eV to be 0.08:0.67:0.25.

We believe the $L_{23}VV$ Auger electrons are largely excited by backscattered secondary electrons since the 1250-1740 eV photons (Mg and Si K_α) can excite many secondary electrons above the 2p Al binding energy around 73 eV [41] as illustrated in Fig. 1. This situation essentially eliminates the asymmetry since the secondary electrons do not "remember" the incoming photon direction.

The L_{23}^2-$L_{23}VV$ satellite results from two processes; namely a cascade process $K \rightarrow L_{23}L_{23} \rightarrow L_{23}VV$ and a shakeoff process $L_{23}^2 \rightarrow L_{23}VV$. The former requires high energy primary electrons to ionize the 1s electrons, and the spherical nature of the 1s orbital eliminates the asymmetry. The shakeoff process in the sudden approximation [42] also requires high energy photons, and now the incoming photon direction will unequally populate the p_x,p_y (p_x,$p_y \propto p_1 \pm p_{-1}$) levels, which will be reflected in the Auger electron yield by the asymmetry. Thus the satellite is excited by the higher energy electrons, and hence the satellite has the higher asymmetry.

An examination of the Auger matrix elements indicates that little d-wave character should be emitted for Al. Performing our own SSC calculations [17b], we find that we can obtain reasonable agreement with the experimental angular distributions without the inclusion of d character, but with an alignment of the p levels; namely with $s:p_z:p_{xy}$ equal to 0:40:60 for the $L_{23}VV$ and 20:40:40 for the L_{23}^2-$L_{23}VV$ patterns. We believe the inclusion of the d-wave by Greber et al was necessary because they did not account for the defocussing effect (i.e. reduced λ) and the possibility for alignment of the p-wave. The negligible s contribution for the $L_{23}VV$ case is consistent with the initial and final state shakeoff process above. The final-state shakeoff process is eliminated in the L_{23}^2-$L_{23}VV$ satellite because now the initial and final states have a core hole.

The strong alignment of the p-wave in the $L_{23}VV$ ARAES again suggests the importance of the backscattered secondary electrons in this case as discussed above. The alignment is strongly reduced in the satellite, because higher energy electrons are needed to dynamically excite the satellite, but now it has higher asymmetry, consistent with Fig. 1.

4.5.Probe directional valence bonds

The Auger amplitudes $B_\ell(m_\ell,m_{\ell'})$ in eq. (1) have been given in terms of the M^2 matrix elements and spin-orbit coupling terms in eq. (4) for free atoms, which we assume is also acceptable for metals. However, in strong covalently bonded materials, spin-orbit coupling is inappropriate, and the M's can better be expressed in terms of the symmetry adapted orbitals n and n' in which the final states holes are located [14],

$$B_\ell(m_\ell,m_{\ell'}) \propto$$

$$| (M_\ell[n,n',m_\ell] \pm M_\ell[n',n,m_\ell]) \qquad (5)$$

$$\times \ (M_\ell[n,n',m_{\ell'}] \pm M_\ell[n',n,m_{\ell'}]) | ,$$

where the plus (minus) is to be taken in case of a singlet (triplet) state.

Now individual peaks in the ERAES lineshape may correspond to particular n,n' combinations which dictates the m_ℓ. For example in a linear diatomic molecule such as CO or LiF, it is best to orient the z-axis along the internuclear bond length, so that particular n,n' combinations will generally yield one m_ℓ state; e.g. σ or π representing very strong alignment or orientation [14]. If the entire Auger intensity is collected regardless of energy, orientation and alignment may still occur because of strongly directed valence bonds particularly near the surface of a solid. We even expect more than one channel (ℓ-wave) to be coherently emitted, such as in diamond exhibiting sp^3 hybridization. In this case bulk atoms will still emit isotropically because all four filled sp^3 hybrid orbitals are oriented symmetrically, but surface atoms may not (i.e. one of the sp^3 hybrids may exist empty as a "dangling" bond).

We believe the above may explain recent data found by Kuettel et al [19] on the C KVV ARAES from diamond (100 and 111) and

graphite (HOPG 0001) surfaces. By fitting SSC calculated results for d and p waves, they found that the diamond "basic structure" was dominated by a d-wave, but the graphite had both d and p-wave character. Assuming electron configurations of sp^3 in diamond and $sp^2\pi^1$ in graphite, we expect Auger contributions of 0.8ss(s) + 3sp(p) + 9pp(d) character, where the first two letters indicate the character of the valence band holes, and the letter in parenthesis indicates the wave character of the dominant Auger electron. Thus we expect a d/p ratio of approximately 3/1 in both carbon solids.

The 1s core level prevents any alignment of the core level, so we need not consider this situation. However, the H-terminated diamond surface under an electron or photon beam is known to desorb H, allowing the surface to reconstruct according to the asymmetric dimer or related model [43]. This reconstruction introduces two effects, namely the directional valence bonds at the surface will be non-isotropic as discussed above, and the p valence band character of the very near surface atoms generally increases [40,43]. The latter effect directly increases the d/p-wave ratio; the former effect should introduce some orientation or alignment of the d- and p-waves and perhaps makes it appear like the isotropic d/p ratio has increased (i.e. similar to Al above).

These diamond surfaces are currently being further studied, but the above results already suggest that ARAES can indeed be used to obtain electronic structure information (as well as atomic structure by AED) at the surface.

4.6.Detect two-center Auger processes

The concept of a two-center Auger process in ionically bonded systems, such as the $M_{23}VV$ process in MgO has existed for many years now [44]. In the completely ionic picture, Mg^{2+} has no valence electrons, so that the 2pVV process must involve electrons from the O^{2-} atom. Although ERAES lineshapes, which reflect the position of the final state holes, are consistent with this picture, does the Auger electron really leave from the O atom, or the Mg atom?

ARAES gives us the chance to actually observe this decay. Chambers and Tran [6] have shown recently that the Mg $L_{23}VV$ and O KVV ARAES polar profiles reveal different structures. The SCC code reproduces these different structures, revealing that the differences arise because of the different scattering behavior of the O atoms vs. the Mg atoms. In Fig. 4 we compare SSC calculated polar profiles with the experimental ones observed by Place and Prutton [18] for the $M_{23}VV$ Mg lineshape. The agreement is poor whether we assume the electron leaves from the O or Mg atom.

One possible explanation for this result is that the $2p_{Mg}$ core hole is screened by charge transfer from the $2p_O$ into the $3s_{Mg}$, which then participates in the Auger decay, i.e. a $2p_{Mg}3s_{Mg}2p_O$ decay. In this case the Auger electron may leave from either the Mg or O atom, depending on which electron falls into the core hole, and which electron enters the detector as the Auger electron. These two processes are indicated by the "direct" and "exchange" matrix elements in eq. (5), and thus Auger waves may be emitted from both centers coherently. Interference of these two waves may create additional oscillations in the "basic structure" of the emitter. Such a process has been theoretically suggested in LiF by Zahringer et al. [14], but no experimental data has been reported to confirm this result in any system. We are currently working to incorporate this phenomenon into the theory; nevertheless, Fig. 4 already reveals that some experimental peaks are evident in the theory for O emission, some in the Mg emission lending strong support for this latter interpretation.

4.7.Estimate orbital magnetic moments

Magnetized metals are known to have their spins aligned, and by the spin-orbit coupling interaction also to possess an orbital magnetic component, i.e. have an orientation in the magnetic d levels [45]. We have previously theoretically investigated the effects on the Auger wave from orientation in

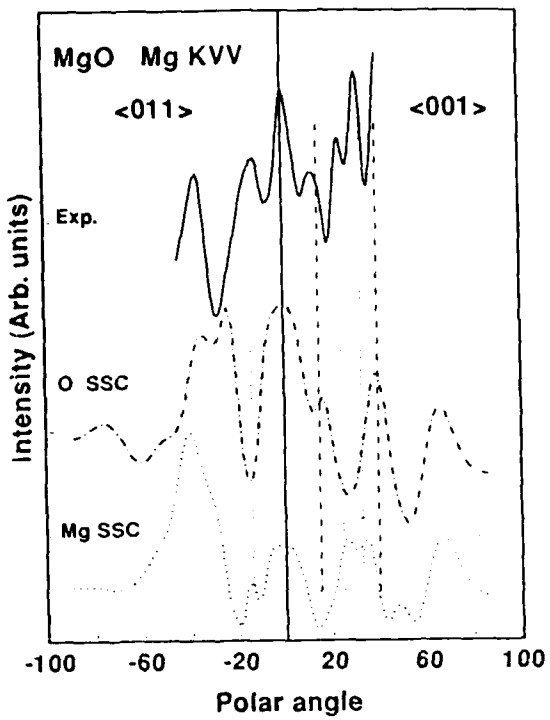

Figure 4. Comparison of the experimental $L_{23}VV$ ARAES polar scans for the MgO (100) surface obtained by Place and Prutton [18] with SSC results obtained with O or Mg as the emitter assuming an s-wave with λ = 12 Å and KE = 27 eV.

the valence levels [17]. In particular we examined the $M_{23}VV$ Auger electrons in Fe. We fixed the quantization axis (the z axis) along the magnetic moment which in thin films can lie normal or parallel to the film. Emission patterns were calculated with the SSC code assuming the emitter is embedded near the (001) surface of a 1500 atom bcc Fe cluster. For the normal moment, a distinct chirality of the spectra was visible; and for the parallel moment, a distinct asymmetry was visible. The chirality or asymmetry in the diffraction pattern is proportional to the orientation, O(3d), in the valence d populations (which directly relates to $<L_z>$), but the exact proportionality constant depends on the scattering, mean free paths of the electrons, Debye-Waller factors, etc. Nevertheless, the prospect exists for obtaining the orbital component of the magnetic moment for surface atoms from ARAES. Such an exciting prospect awaits experimental confirmation, and further theoretical development.

5.CONCLUSIONS

We conclude ARAES may be a useful tool to study various electronic processes. We have outlined several interesting prospects, some realized, some requiring further development and verification. The interest in angle resolved data has occurred primarily because of the demonstrated ability to obtain atomic structure information on films and surfaces (the latter we call AED); but the potential information obtainable from ARAES may be equally helpful. Much further development of the theory is necessary to make these goals become realized. Further development of the theory outlined here would also improve the atomic structure information obtainable in AED.

REFERENCES

1. W.F. Egelhoff, Jr., Crit. Rev. Solid Mater. Sci. 16 (1990) 213; and ref. therein.
2. C.S. Fadley, Prog. Surf. Sci. 16 (1984); Synch. Rad. Res., Adv. in Surf. Sci., ed. R.Z. Bachrach (Plenum, NY, 1990).
3. S.A. Chambers, Adv. in Phys. 40 (1991) 357; Surf. Sci Report 16 (1992) 261.
4. T. Greber, J. Osterwalder, D. Naumovic, A. Struck, S. Hufner, and L. Schlapbach, Phys. Rev. Lett. 69 (1992) 1967; Surf. Sci 269 (1992) 719; Phys. Rev. 45 (1992) 4540.
5. Y.U. Idzerda and G.A. Prinz, Surf. Sci. Lett. 284 (1993) L394.
6. S.A. Chambers and T.T. Tran, Phys. Rev. B, Surf. Sci. 314 (1994) L867.
7. S. Valeri and A. DiBona, Nuovo Cimento 16(5), 1 (1993).
8. H.P. Bonzel, Prog. Surf. Sci. 42, 219 (1993).
9. L. McDonnell, D.P. Woodruff, B.W. Holland, and S. J. White, Surf. Sci. 51 (1975) 249; 72 (1978) 77.

10. R.N. Lindsay and C.G. Kinniburgh, Surf. Sci. 63 (1977) 162.
11. T. Matsudaira, M. Nishijima, and M. Onchi, Surf. Sci. 61 (1976) 651; 72 (1978) 53; 74 (1978) 684; Sol. State Commun. 29 (1979) 549.
12. D.M. Zehner, J.R. Noonan, and L.H. Jenkins, Sol. State Commun. 18 (1976) 483; 69 (1977) 731; J. Vac. Sci. Technol. 13 (1976) 183; H.L Davis and T. Kaplan, Sol. State Commun. 19 (1976) 595.
13. R. Baudoing, G. Allie, E. Blanc, C. Gaubert, Y. Gauthier and D. Aberdam, Surf. Sci 128 (1983) 22; 71 (1978) 279; 57 (1976) 306; 57 (1976) 293; also in: Physics of Solid Surfaces, Ed. M. Laznicka (Elsevier, Amsterdam, 1982) 87-111.
14. K. Zahringer, H.D. Meyer, and L.S. Cedarbaum, Phys. Rev. A46 (1992) 5643.
15. Y.U. Idzerda and D.E. Ramaker, Phys. Rev. Lett. 69 (1992) 1943.
16. J.J. Barton and L.J. Terminello, Phys. Rev. B46 (1992) 11548; 47 (1993) 6851.
17. D.E. Ramaker, H. Yang, and Y.U. Idzerda, J. Electron Spectrosc. Related Phenom. 68 (1994) 63; Mater. Res. Soc. Symp. Proc. 295 (1993) 225; 313 (1993) 659.
18. J.D. Place and M. Prutton, Surf. Sci. 82 (1979) 315.
19. O.M. Kuettel, R.G. Agostino, R. Fasel, J. Osterwalder, and L. Schlapbach, Surf. Sci. 312 (1994) 132.
20. A. Stuck, M. Nowicki, S. Mroz, D. Naumovic, J. Osterwalder, Surf. Sci. 306 (1994) 21; 297 (1993) 66.
21. D.J. Friedman and C.S. Fadley, J. Electron Spectrosc. Relat. Phenom. 51 (1990) 689; A.P. Kaduwela et al, Phys. Scr. 41 (1990) 948.
22. R.N. Zare, Angular Momentum (John Wiley & Sons, NY, 1988).
23. E.G. Berezhko and N.M. Kabachnik, J. Phys. B10 (1977) 2467; 11 (1978) 1819.
24. H. Klar, J. Phys. B13 (1980) 2037; 4741.
25. U. Hahn, J. Semke, H. Merz, and J. Kessler, J. Phys. B18 (1985) L417.
26. W. Sander and V. Schmitt, J. Phys. B. 11 (1978) 1833; W. Mehlhorn, Nucl. Instrum. Methods Phys. Res. B87 (1994) 227.
27. E.G. Berezhko and N.M. Kabacknik, J. Phys. B 13 (1980) 959; M. Benhenni et al, Nucl. Instrum. Methods Phys. Res. B86 (1994) 28.
28. N.M. Kabacknik and O.V. Lee, J. Phys. B. 22 (1989) 2705.
29. U. Heinzmann et al, Phys. Rev. Lett. 70 (1993) 3716; Phys. Scripta T41 (1992) 190; A. Hausmann et al, Phys. Rev. Lett. 61 (1988) 2669; V. Schmidt, Nucl. Instrum. Methods Phys. Res., B87 (1994) 241; M. Phaler, AIP Conf. Proc. 295 (1993) 93.
30. N.M. Kabachnik et al, J. Phys. B 11 (1978) 1749; 14 (1981) L337; 17 (1984) 1335; 21 (1988) 267; 3695; 23 (1990) L353; Phys. Lett A66 (1978) 474; AIP Conf. Proc. 295 (1993) 73.
31. J.M. Plociennik, A. Barbet, and L. Mathey, Surf. Sci. 102 (1981) 282.
32. S.P. Weeks and A. Liebsch, Surf. Sci. 62 (1977) 197.
33. Since the SSC code is limited to $m_\ell \leq 3$, the $m_\ell = \pm 4$ contributions in the g wave are not included here; but these levels contribute primarily beyond the angle range in Fig. 2 anyway.
34. M. Scrocco, Phys. Rev. B29 (1984) 1722.
35. Y. Sakisaka, T.N. Rhodin, and P.A. Dowben, Sol. State Commun. 49 (1984) 563.
36. S. Mroz and B. Stachnik, Surf. Sci. 247 (1991) 201; Sol. State Phenom. 12 (1990) 139;
37. E.N. Sickafus and C. Kukla, Phys. Rev. B19 (1979) 4056.
38. E.D. Roberts, P. Weightman, C.E. Johnson, J. Phys. C8 (1975) L301.
39. D.E. Ramaker, Crit. Rev. Solid State Mater. Sci. 17 (1991) 211.
40. D.E. Ramaker, F.L. Hutson, N.H. Turner, W.N. Mei, Phys. Rev. B33 (1986) 2574.
41. A. Jablonski, Surf. Sci. 87 (1979) 539.
42. J. Stohr, R. Jaeger, and J.J. Rehr, Phys. Rev. Lett. 51 (1983) 821; T.D. Thomas, Phys. Rev. Lett. 52 (1984) 417.
43. D.E. Ramaker et al, Solid State Commun. 63 (1987) 335.
44. M. Salmeron, A.M. Baro, and J.M. Rojo, Surf. Sci. 53 (1975) 689; 79 (1978) 77; V.M. Bermudez and V.H. Ritz, Surf. Sci. 82 (1979) L601.
45. O. Eriksson et al, Phys. Rev. B42 (1990) 2707.